

See discussions, stats, and author profiles for this publication at: <https://www.researchgate.net/publication/277348486>

Heterogeneous Photocatalysis and Photoelectrocatalysis: From Unselective Abatement of Noxious Species to Selective Production of High-Value Chemicals

ARTICLE *in* JOURNAL OF PHYSICAL CHEMISTRY LETTERS · APRIL 2015

Impact Factor: 7.46 · DOI: 10.1021/acs.jpclett.5b00294

CITATIONS

2

READS

65

7 AUTHORS, INCLUDING:



Giovanni Camera-Roda

University of Bologna

43 PUBLICATIONS 649 CITATIONS

[SEE PROFILE](#)



Giovanni Palmisano

Masdar Institute of Science and Technology

76 PUBLICATIONS 2,138 CITATIONS

[SEE PROFILE](#)



Leonardo Palmisano

Università degli Studi di Palermo

263 PUBLICATIONS 10,563 CITATIONS

[SEE PROFILE](#)



Javier Soria

Spanish National Research Council

228 PUBLICATIONS 7,033 CITATIONS

[SEE PROFILE](#)

Heterogeneous Photocatalysis and Photoelectrocatalysis: From Unselective Abatement of Noxious Species to Selective Production of High-Value Chemicals

Vincenzo Augugliaro,[†] Giovanni Camera-Roda,[‡] Vittorio Loddo,[†] Giovanni Palmisano,[§]
Leonardo Palmisano,^{*,†} Javier Soria,^{||} and Sedat Yurdakal[⊥]

[†]Schiavello-Grillone Photocatalysis Group, Dipartimento di Energia, ingegneria dell'Informazione e modelli Matematici (DEIM), University of Palermo, Viale delle Scienze, 90128 Palermo, Italy

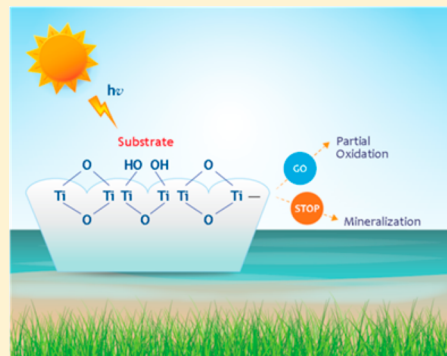
[‡]Dipartimento di Ingegneria Civile, Chimica, Ambientale e dei Materiali (DICAM), University of Bologna, via Terracini 28, 40131 Bologna, Italy

[§]Department of Chemical and Environmental Engineering, Institute Center for Water and Environment (iWater), Masdar Institute of Science and Technology, PO Box 54224, Abu Dhabi, United Arab Emirates

^{||}Instituto de Catálisis y Petroleoquímica, Consejo Superior de Investigaciones Científicas (CSIC), C/Marie Curie 2, Cantoblanco, 28049 Madrid, Spain

[⊥]Kimya Bölümü, Fen-Edebiyat Fakültesi, Afyon Kocatepe Üniversitesi, Ahmet Necdet Sezer Kampüsü, 03200 Afyon, Turkey

ABSTRACT: Heterogeneous photocatalysis and photoelectrocatalysis have been considered as oxidation technologies to abate unselectively noxious species. This article focuses instead on the utilization of these methods for selective syntheses of organic molecules. Some promising reactions have been reported in the presence of various TiO₂ samples and the important role played by the amorphous phase has been discussed. The low solubility of most of the organic compounds in water limits the utilization of photocatalysis. Dimethyl carbonate has been proposed as an alternative green organic solvent. The recovery of the products by coupling photocatalysis with pervaporation membrane technology seems to be a solution for future industrial applications. As far as photoelectrocatalysis is concerned, a decrease in recombination of the photogenerated pairs occurs, enhancing the rate of the oxidation reactions and the quantum yield. Another benefit is to avoid reaction(s) between the intermediates and the substrate, as anodic and cathodic reactions take place in different places.



A large number of articles, reviews, books, and patents deal with pollutants abatement by heterogeneous photocatalysis and photoelectrocatalysis.^{1–9} Most studies on wastewater treatment refer to different categories of noxious pollutants such as pesticides, dyes, drugs, and their intermediates. In most of the applications of photocatalysis, only the capability of the catalysts (usually TiO₂) to degrade organic species has attracted attention. Heterogeneous photocatalysis has been considered a very interesting advanced oxidation technology for water or air purification because very few compounds are refractory to photocatalytic oxidation, even the most recalcitrant to biological treatment.

However, photocatalysis is capable also of partial or selective oxidation and reduction to produce high value chemicals from various substrates.^{10–14} Selective photocatalytic and photoelectrocatalytic reactions could offer alternative green routes to organic syntheses that currently are carried out by using harmful reagents/catalysts or under drastic or environmentally unfriendly conditions.

Some pioneering papers reported the use of heterogeneous photocatalysis to synthesize different products, for instance,

Selective photocatalytic and photoelectrocatalytic reactions could offer alternative green routes to organic syntheses that currently are carried out by using harmful reagents/catalysts or under drastic or environmentally unfriendly conditions.

cyclic amino acids,¹⁵ cyclohexanol, and cyclohexanone from cyclohexane^{16,17} and imines from amines.¹⁸ The conversion of adamantane to 1- and 2-adamantanol and adamantanone under UV light¹⁹ and synthesis of some heterocyclic aldehydes from some heterocyclic bases with ethers induced by sunlight²⁰ are

Received: February 10, 2015

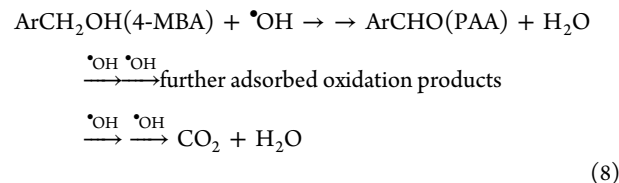
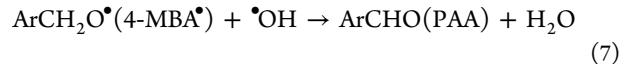
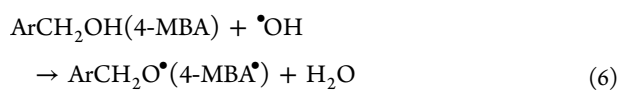
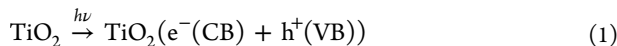
Accepted: April 30, 2015



present in the literature. Selective oxidation of aliphatic and aromatic alcohols has been carried out both in the gas phase²¹ or by using acetonitrile as the solvent.²²

In the present paper, some selected promising cases reported in the recent literature will be briefly illustrated, regardless of whether or not they meet all of the principles of Green Chemistry.²³ The presented examples (many have been investigated by the authors) concern reacting systems in which safer chemicals and milder operative conditions have been used in comparison with those usually adopted in the traditional syntheses.^{12,13} Yet, the recovery and the purification of the products is another important problem that can be advantageously faced by the integration of the reaction with a membrane separation process.²⁴

Aromatic Alcohol Partial Oxidation. The oxidation of aromatic alcohols to aromatic aldehydes is of particular relevance among the selective reactions. 4-Methoxybenzaldehyde (*p*-anisaldehyde, PAA) has been produced by the photocatalytic selective oxidation of 4-methoxybenzyl alcohol (4-MBA) in aqueous (additive-free) suspensions of TiO₂.²⁵ PAA is used in confectioneries and beverages, and its industrial synthetic route involves the oxidation of *p*-cresyl methyl ether by manganese dioxide and sulfuric acid. It was demonstrated that the properties of home prepared (HP) photocatalyst strongly affect the yield. Nanostructured HPX samples were synthesized under mild conditions by boiling aqueous solutions of TiCl₄ for different times, where X indicates the boiling time in hours. The crystallinity increased with the boiling time, but the highest selectivity (42%) to PAA was found for the least crystalline sample (boiled 0.5 h, anatase), although the 4-MBA oxidation rate followed the same pattern. A comparison with the two commercial TiO₂ samples, Merck (100% anatase) and Degussa P25 (P25, 80% anatase, 20% rutile), showed that all the HP photocatalysts exhibited higher selectivities and yields than the commercial ones. Subsequent studies have been carried out by using a configuration of the system, which is more suitable for application purposes. A HP TiO₂ photocatalyst was prepared by calcining the precursor at 400 °C for 3 h on Pyrex glass beads and was used in a continuous annular fixed-bed photoreactor.^{26,27} The reactivity results showed that the photocatalytic oxidation of 4-MBA took place through two parallel routes that are effective from the beginning of irradiation: the first is a partial oxidation producing PAA, and the second one leads to mineralization. The partial oxidation pathway was favored by low photon fluxes and low oxygen coverage of the TiO₂ surface. Below, a mechanism is reported, describing the transformation of a generic aromatic alcohol to the corresponding aldehyde, which desorbs into the bulk of the solution



The possibility to produce PAA from 4-MBA is highlighted in brackets, as an example. On the other hand, eq 8 indicates the possibility that some of the aldehydes produced by the partial oxidation and other products remain strongly adsorbed while they undergo a fast oxidation until complete mineralization. The occurrence of two parallel pathways suggests that the TiO₂ surface is endowed with two types of sites that are specific for the occurrence of mineralization or partial oxidation. The identification of the different sites is very difficult; anyhow, it has been observed that CO₂ develops soon after irradiation together with the appearance of the desorbed products.²⁸

Rutile TiO₂ photocatalysts generally show a lower activity than anatase and are usually prepared by anatase calcination at high temperatures.²⁹ Nevertheless, preparations of rutile at low temperatures with an appreciable photoactivity have been reported³⁰ and HP samples of rutile TiO₂ have been successfully used in water free of any organic cosolvent for the oxidation of benzyl alcohol (BA) and 4-MBA to benzaldehyde (BAD) and PAA, respectively.³¹ Small amounts of hydroxylated benzaldehydes and benzoic acid together with BAD and CO₂ were obtained only during BA oxidation.^{31,32} The low temperature rutile preparation was carried out by a sol-gel route. A white sol generated by TiCl₄ hydrolysis in water was kept in an oven for 2 days at 333 K. Then, the suspension was dried at 333 K to obtain the final powdered TiO₂ (HP333). To check the influence of the degree of crystallinity on the reactivity, HP333 was calcined at 673 and 973 K (HP673 and HP973). In Table 1, the behavior of some HP rutile samples prepared according to this method is compared with a commercial rutile sample (Sigma-Aldrich). The best selectivity in BAD and PAA was obtained with HP333, indicating that a low degree of crystallinity is sufficient to induce the photo-oxidation with high selectivity. Notably, totally amorphous samples (not reported in Table 1) showed negligible photoactivity. In light of these results, two questions arise: Besides the structural properties, are the intrinsic electronic properties important? What is the role of the surface physicochemical properties?

In light of these results, two questions arise: Besides the structural properties, are the intrinsic electronic properties important? What is the role of the surface physicochemical properties?

To get an answer, though tentatively, to the previous questions, the photoelectrochemical features of selected anatase and anatase/rutile HP samples (prepared according to ref 25 and used to carry out the 4-MBA photocatalytic oxidation) were determined by diffuse reflectance spectroscopy and quasi-Fermi level measurements.³³

Table 1. BET Specific Surface Area, Crystallite Size, and Photocatalytic Performance of Selected Photocatalysts^{a,34}

	SSA [$\text{m}^2 \cdot \text{g}^{-1}$]	crystallite size [nm]	catalyst amount [$\text{g} \cdot \text{L}^{-1}$]	$t_{1/2}$ [h] ^b	selectivity [%] ^b
homogeneous system					
HP333	107	7	0.20	176	14
HP333	107	7	0.40	17	38
HP333	107	7	0.60	8.4	38
HP333–4-MBA	107	7	0.40	9.0	38
HP673	35	13	0.40	2.4	60
HP973	4	41	0.40	6.0	12
Sigma-Aldrich	2.5	52	0.40	9.4	9.9
Sigma-Aldrich-4-MBA	2.5	52	0.40	3.8	9.2
				2.2	21

^aThe results refer to BA oxidation except those for HP333–4-MBA and Sigma-Aldrich-4-MBA referring to 4-MBA oxidation. ^bIrradiation time and selectivity were calculated for an alcohol conversion of 50%. Selectivity = (produced PAA moles)/(converted 4-MBA moles) × 100.

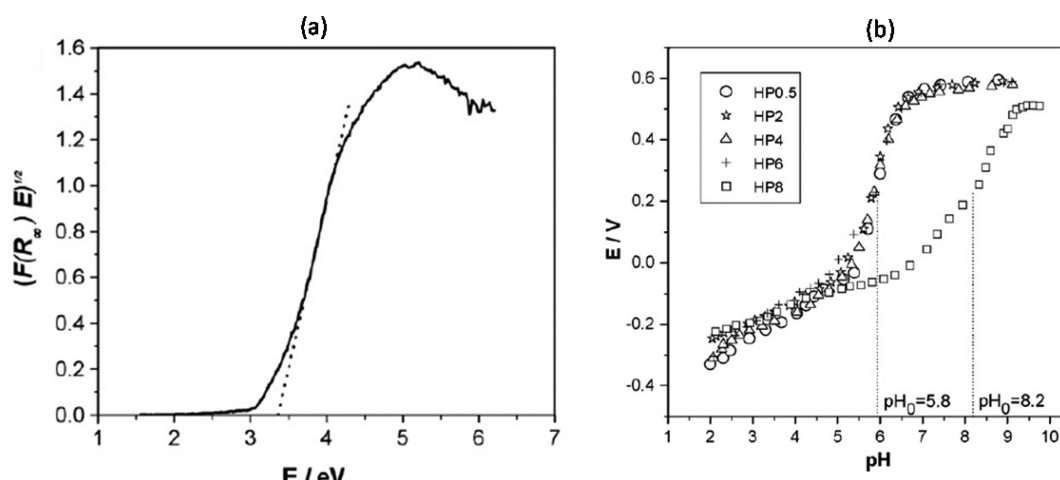


Figure 1. (a) Diffuse transformed reflectance spectra of HP0.5 sample. (b) Variation of photovoltage with pH value. A total of 50 mg of catalyst and 10 mg of methyl viologen dichloride are suspended in 50 mL of 0.1 M KNO_3 aqueous solution at room temperature. Pt is the working electrode, and Ag/AgCl is the reference electrode.³³ Reprinted with permission. Copyright 2008, Elsevier.

The technique reported by Roy et al.³⁴ allowed determination of the flat band potential, E_{fb} , of CdS and CdS/Ag₂S (1.5 wt %) particles from photovoltage measurements in the presence of the electron acceptor methyl viologen (MV^{2+}). Measurements were made while irradiating the semiconductor suspensions with visible light. By assuming that the difference between the quasi-Fermi level potential and conduction band edge is negligible, the valence band edge values can be obtained by addition of the band gap energy. Figure 1 shows the diffuse transformed reflectance spectra (determination of band gap) and the variation of photovoltage with pH value (quasi-Fermi level measurements) for HPX samples. Table 2 shows the photoelectrochemical

properties of the HP samples and two commercial TiO₂ samples Merck and Degussa P25, along with their selectivity to PAA.

HP0.5, HP2, and HP4 band edge are located at 2.84 V, whereas those of HP6 and HP8 samples are shifted to 2.74. HP6 contains a significant amount of rutile (anatase being the predominant phase), whereas HP8 is nearly pure rutile. The values of band gap, valence band, and conduction band edges are almost identical for all of the HP anatase samples, whereas appreciable differences can be noted for an HP sample containing or consisting of rutile phase. Consequently, the differences in selectivity observed especially for the anatase samples (see Table 2) cannot be straightforwardly related to the values of band gap, E_{fb} , and VB edge.

In order to understand if the surface properties play a role, a comparative ATR-FTIR study of HP0.5 and P25 samples was carried out. Figure 2 shows time-resolved ATR-FTIR spectra of these samples recorded after adsorption of water (see bands at 1640, 3400, and 3240 cm^{-1}) and BA vapors. For HP0.5 (Figure 2, a), molecular BA appears to be the predominant surface organic species formed. Alcoholates were not detected by FT-IR, whereas—as far as P25 is concerned (Figure 2, b)—a group of absorptions at 1413, 1340, and 1156 cm^{-1} are detected. The band centered at 1156 cm^{-1} might be ascribed to a C—O stretching vibration; its blue shift with respect to the molecular alcohol is large enough to indicate the formation of adsorbed benzolate species.

The ATR-FTIR results indicate that HP0.5 and P25 surfaces show a very dissimilar hydrophilicity and different ability to

Table 2. Some Properties of HP Catalysts and Two Commercial Samples^{33,35}

catalyst	band gap [eV]	E_{fb} (pH 7) [V]	VB edge [V]	SSA [$\text{m}^2 \cdot \text{g}^{-1}$]	selectivity (mol) [%] ^a
P25 (A, R)	3.26	-0.55	2.71	50	8.7
Merck (A)	3.22	-0.43	2.79	10	12
HP0.5 (A)	3.36	-0.52	2.84	235	42
HP2 (A)	3.36	-0.52	2.84	226	37
HP4 (A, R)	3.36	-0.52	2.84	220	36
HP6 (A, R)	3.26	-0.52	2.74	206	31
HP8 (R)	3.11	-0.37	2.74	108	32

^aInitial pH of the suspension = 7, selectivity (%) calculated after a conversion of ca. 65% of the initial alcohol, quantity of catalyst = 0.2 g. In HPX, X indicates the boiling time.

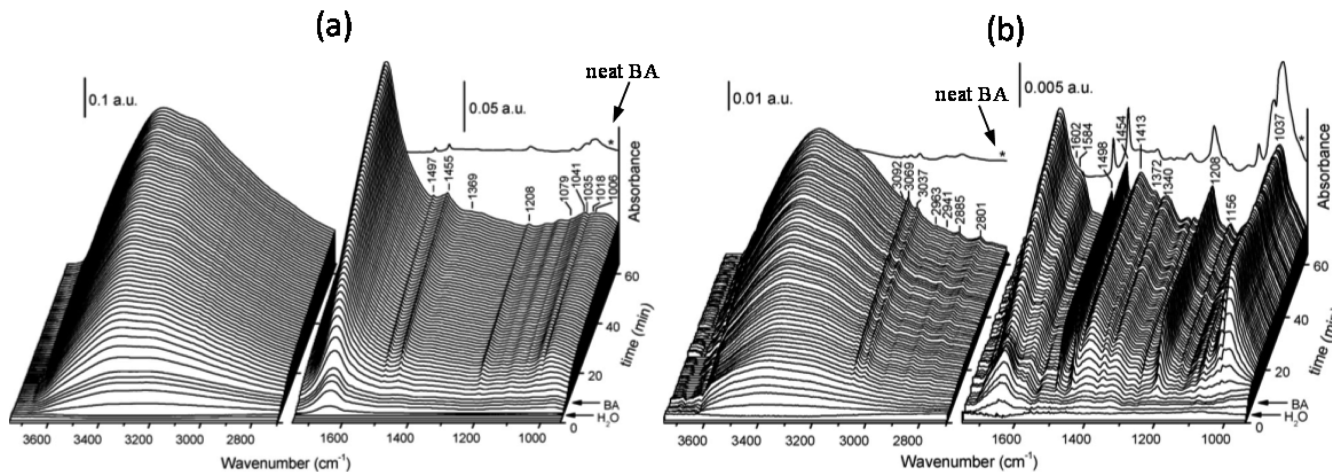


Figure 2. Time resolved ATR-FTIR spectra of HP0.5 (a) and Degussa P25 (b) thin films recorded during adsorption of water and BA vapors at room temperature. The arrows indicate the time when each adsorbate was introduced in the cell. The spectrum of neat BA (*) multiplied by a factor of 0.01 has been included for comparison.³³ Reprinted with permission. Copyright 2008, Elsevier.

Table 3. BET Specific Surface Area SSA, Band Gap Energy E_g , Particle Size, Crystallite Size of Photocatalysts and Their Photocatalytic Performance for 4-MBA Photo-Oxidation to PAA for 50% Conversion^a

catalyst	SSA [m ² ·g ⁻¹]	E_g [eV]	aging time [days]	agglomerate size [nm]	crystallite size [nm]	catalyst amount [g·L ⁻¹]	$t_{1/2}$ [h]	selectivity [% mol]	C balance [%]
HP1/20	129	3.32	9	286	5.5	0.2	2.3	45	91
HP1/35	116	3.33	6	1050	5.6	0.6	3.6	60	96
HP1/50	118	3.36	6	719	6.8	0.2	6.7	74	99
HP1/50	118	3.36	6	719	6.8	0.6	2.6	72	98
HP1/75	125	3.33	4	304	7.1	0.2	3.0	55	94
HP1/100	135	3.36	4	244	6.1	0.2	3.3	61	96
Sigma-Aldrich	2.5			240	52	0.4	2.2	21	70

^aC balance was obtained as sum of 4-MBA, PAA, and CO₂ concentration.

adsorb BAD. Indeed, the HP0.5 reactivity results show a low oxidation rate of BA but a high selectivity toward BAD, as the HP0.5 surface is rich in molecularly adsorbed water, which is able to displace BA molecules in the dark. Under irradiation (spectra not shown), water displaces BA and the produced BAD more effectively, determining a very low oxidation rate of BA and a higher selectivity. On the contrary, in the case of P25, the reactivity results indicate that the mineralization pathway predominates over the partial oxidation. The lower hydrophilicity of P25 as compared to HP0.5 implies a low ratio between water and benzyl alcohol, and therefore, it is likely that mineralization sites are not preferentially occupied by water molecules.^{33,36}

TiO₂ rutile samples were also prepared under very mild conditions at room temperature simply by using TiCl₄ as the TiO₂ precursor without any additive.²⁸ Different volumetric ratios of TiCl₄ to H₂O were used to carry out the TiCl₄ hydrolysis for some days (samples name refers to the TiCl₄ to H₂O ratio, HP1/20 ÷ HP1/100). Table 3 shows results of physical characterization and performances of the different samples. The highest selectivity (up to 74%) and C balance values (99%) for PAA formation were obtained by using HP1/50, whereas the worst ones were obtained with Sigma-Aldrich TiO₂.

The importance of the position of the substituent groups in aromatic alcohols was also studied.³⁷ BA, 2-methoxybenzyl alcohol (2-MBA), 3-methoxybenzyl alcohol (3-MBA), 4-methoxybenzyl alcohol (4-MBA), 2,4-dimethoxybenzyl alcohol (2,4-DMBA), 4-hydroxybenzyl alcohol (4-HBA), and 3-methoxy-4-hydroxybenzyl alcohol (3M,4-HBA) have been photocatalytically

Table 4. Results of Photocatalytic Oxidation of Benzyl Alcohol Derivatives to Their Corresponding Aldehydes by Using 0.20 g·L⁻¹ HP1/50 and 0.50 g·L⁻¹ Sigma-Aldrich^a

substrate	$-r_0 \cdot 10^6$ [mM mh ⁻¹]	selectivity [%]	$t_{1/2}$ [h]	C balance [%]	min [%]
HP1/50 Catalyst					
BA	3.44	13	10	91	78
2-MBA	17.2	50	2.7	99	49
3-MBA	7.38	28	5.0	89	61
4-MBA	16.6	59	2.1	90	31
2,4-DMBA	22.6	58	0.9	86	28
4-HBA	4.64	8.0	7.2	99	91
3M,4-HBA	7.57	1.0	4.0	85	84
Sigma-Aldrich Catalyst					
BA	113	5.0	6.3	36	31
2-MBA	194	14	3.0	68	54
3-MBA	168	6.0	4.6	68	62
4-MBA	191	25	3.8	83	58
2,4-DMBA	204	20	2.2	58	38
4-HBA	81.9	5.0	8.3	67	62
3M,4-HBA	114	2.2	4.5	57	55

^aInitial degradation rate, r_0 ; mineralization percentage of reacted substrate, min. Selectivity, C-balance, and min values were calculated for 70% conversion.

oxidized to their corresponding aldehydes in aqueous TiO₂ suspensions under near-UV irradiation (Table 4). The selectivity decreased with the substituent position on the aromatic ring according to the following order: para > ortho > meta. In the

Table 5. Crystalline Phase, Band Gap Energy E_g , Crystallinity, BET Specific Surface Area SSA, Agglomerate Size and Crystallite Size of the Catalysts, and Their Photocatalytic Performance for the Oxidation of HMF to FDC^a

catalyst sample	crystalline phase ^b	E_g [eV]	crystallinity [%]	$r_0 \cdot 10^6$ ^c [mM·m·h ⁻¹]	$t_{1/2}$ ^d [h]	selectivity ^e [%]
Sigma-Aldrich	R		100	181	3.5	11
Merck	A	3.22	74	62	2.6	13
P25	A:R (80:20%)	3.26	90	28	1.2	12
HPB	B			8.2	2.6	21
HP1/50	R	3.36	13	2.2	13	25
HP2	A	3.36	2.9	2.4	4.0	23
HP2 ^f	A	3.36	2.9	0.6	16	26

^aCatalyst amount, 0.20 g·L⁻¹; initial concentration of HMF, 0.50 mM. ^bA, anatase; R, rutile; B, brookite. ^cInitial reaction rate. ^dIrradiation time needed to reach a HMF conversion of 50%. ^eSelectivity values were calculated for 20% of conversion. ^fRun performed in the presence of 50 mM methanol.

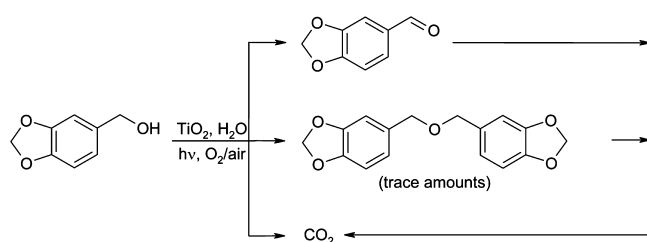
presence of two substituent groups, the overall oxidation rate increased while the selectivity decreased. HP1/50 generally showed higher selectivity but lower activity (reaction rate per unit surface area) than Sigma-Aldrich TiO₂.

Photocatalytic oxidation of 4-MBA to PAA in water and under UV irradiation was also carried out by using a two-step preparation of polystyrene/anatase TiO₂ core/shell colloidal particles.³⁸ Both the samples, with and without thermal treatment (3 h at 450 °C), were found more selective (70 and 64%, respectively) for PAA production than the Merck one (21%).

The first photocatalytic synthesis of 2,5-furandicarbaldehyde (FDC) from 5-(hydroxymethyl)-2-furaldehyde (HMF) has been performed in aqueous medium by using home prepared (HP) anatase, rutile and brookite TiO₂ nanoparticles.³⁹ The results showed that with HP catalysts the selectivities toward FDC were more than twice than those of the commercial samples (see Table 5). However, commercial samples were more active (reaction rate per unit surface area) than HP ones.

Piperonal is another aldehyde synthesized in aqueous suspensions of home-prepared TiO₂.⁴⁰ Badly crystallized catalysts of both anatase and rutile TiO₂ gave selectivities ranging between 10 and 19% after a conversion of 30% (although higher selectivities up to 84% were obtained for lower conversions), whereas commercial TiO₂ allowed reaching a selectivity of only ca. 6%. The other products of the photoprocess were 1,3-bis(3,4-(methylenedioxy)benzyl)ether (found in traces) and CO₂, derived from photomineralization. Scheme 1 shows the hypothesized mechanism.

Scheme 1. Main reaction pathways of synthesis of piperonal.⁴⁰ Reprinted with permission. Copyright 2014, Elsevier



Another example of successful partial oxidation was the synthesis of vanillin from *trans*-ferulic acid, eugenol, isoeugenol, or vanillyl alcohol by using both commercial and HP TiO₂ samples.⁴¹ Table 6 reports the values of the highest selectivity to vanillin obtained under different irradiation times from runs carried out with different substrates.

HP photocatalysts were more selective than the commercial ones when vanillyl alcohol was used. An opposite behavior was observed for the other three substrates: commercial TiO₂ photocatalysts showed to be more selective than the HP ones. Scheme 2 shows the reaction pathways for *trans*-ferulic acid; unidentified or unstable species are reported in square brackets.

As a general behavior for all of the investigated processes, the reaction selectivity decreased as the conversion increased. The main reason for this phenomenon is that the produced aldehyde decreases by further oxidation, which is a consequence of the photocatalytic activity in the reactor.

It is advisable to recover the aldehyde while it is formed in order to prevent its degradation. To this aim, a membrane process, namely pervaporation, has been coupled to the photocatalytic reaction.

Therefore, it is advisable to recover the aldehyde while it is formed in order to prevent its degradation. To this aim, a membrane process, namely pervaporation, has been coupled to the photocatalytic reaction.^{42–44} The utilized nonporous membrane in PEBA (poly-ether-block-amide) showed to be very selective toward vanillin with respect to most of the other organic compounds that are present in the reacting solution, and it is able to completely retain the photocatalytic powders.⁴³ Figure 3 shows the almost pure vanillin crystals (ca. 99.9% purity) obtained by pervaporating the reacting solution.

Indeed, pervaporation showed to be a very suitable separation process for the coupling with photocatalysis. The two processes are highly compatible since they can operate at the same conditions and the integration is simple and straightforward even operating with separate pieces of equipment.⁴³ With the integrated process, the recovery of vanillin during its production has the effect of highly enhancing the selectivity because the further oxidation of vanillin is thus prevented. In some cases, the yield in vanillin with the integrated process can increase up to 200–300% if the area of the membrane is optimized.

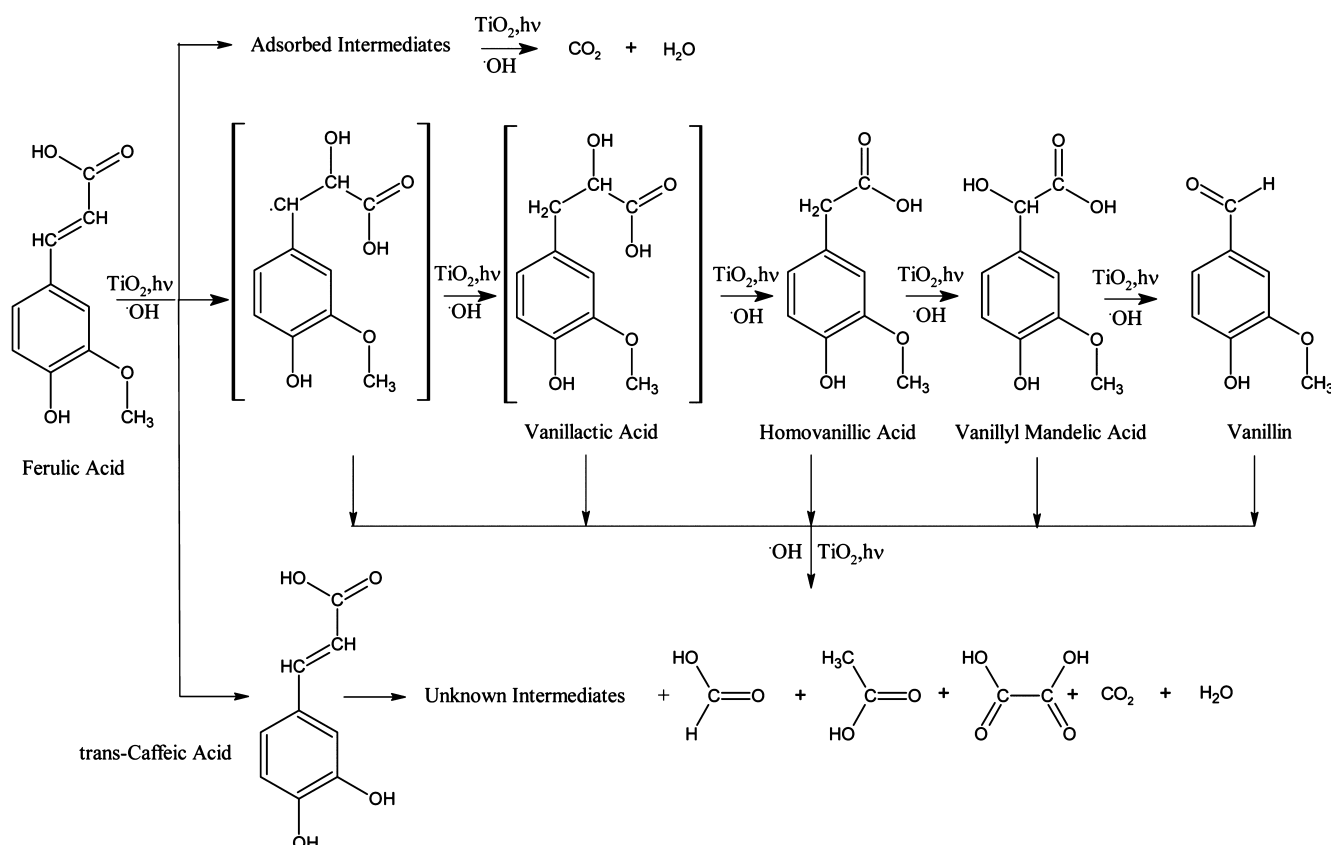
In order to efficiently utilize sun light for aromatic alcohol synthesis in water, N-doped TiO₂ catalysts were also investigated.^{45–47} N-doped anatase–rutile photocatalysts were prepared by a sol-gel method, using TiCl₄ as TiO₂ precursor and urea as N-doping source.⁴⁷ The photocatalytic activity of the samples was tested for the partial oxidation of 4-MBA to

Table 6. Irradiation Time t_{irr} , Conversion X, and Selectivity to Vanillin S for Runs Carried out by Using Different TiO_2 Photocatalysts in the Presence of Pure Oxygen or Air

catalyst	gas type	<i>trans</i> -ferulic acid			isoeugenol			eugenol			vanillyl alcohol		
		t_{irr} [min]	X [%]	S [%]	t_{irr} [min]	X [%]	S [%]	t_{irr} [min]	X [%]	S [%]	t_{irr} [min]	X [%]	S [%]
P25	O_2	15	10	3	30	94	6.5	15	41	2.6	30	40	9
	air	30	11	3	90	84	9.2	60	43	2.8	30	17	16
Merck	O_2	60	18	8	90	56	9.6	60	37	2.7	30	14	15
	air	90	14	12	90	54	12	60	20	5	60	19	14
HPC3 ^a	O_2	60	98	1.5							60	16	13
	air	90	42	2	15	27	8.3	30	23	3.5	90	15	21
HP0.5	O_2	60	97	1.6							60	11	20
	air	120	96	1.4	15	71	1.5	15	30	1.2	120	13	16

^aHome prepared sample consisting of badly crystallized rutile phase.

Scheme 2. Proposed reaction pathways for *trans*-ferulic acid photo-oxidation^{41 a}



^aReprinted with permission.⁴¹ Copyright 2012, Elsevier.

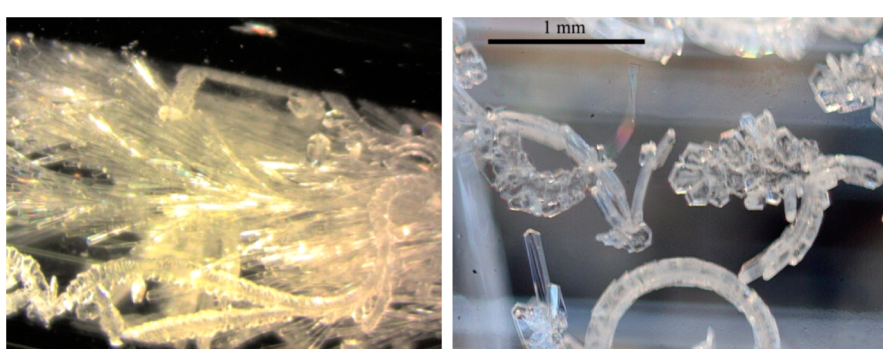


Figure 3. Vanillin crystals obtained by fractional condensation of permeate vapors in pervaporation.^{41,43} Reprinted with permission. Copyright 2012/2013, Elsevier.

Table 7. Results of Photocatalytic Oxidation of Glycerol Obtained with the APR and the CPR, Band Gap Energies E_g , Reaction Time Required for 35% Conversion $t_{35\%}$, and Selectivities S Towards the Known Products^a

catalyst	E_g [eV]	reactor type	catalyst amount [g/L]	$t_{35\%}$ [h]	S_{GAD} [%]	S_{DHA} [%]	S_{FA} [%]	S_{CO_2} [%]
homogeneous		APR		17 ^b	4.5 ^b	3.7 ^b	6.5 ^b	
P25	3.26	APR	0.100	25	7.0	4.0	3.0	17
Sigma-Aldrich		APR	0.400	31	10.5	5.2	10	24
HP1/50	3.36	APR	0.200	30	4	2.5	3.7	11
HP0.5	3.36	APR	0.300	32	6.5	5	7.4	21
homogeneous		CPR		13 ^b	13 ^b	7.2 ^b	7.0 ^b	
P25	3.26	CPR	0.046	12	8	6.2	6.3	29
P25	3.26	CPR	0.091	10	10	7	8.8	27
P25	3.26	CPR	0.182	13	8	7	6.8	31
Sigma-Aldrich		CPR	0.091	7.7	9.5	4.5	8	7.1
HP1/50	3.36	CPR	0.091	11	6.5	4.6	5.5	29
HP0.5	3.36	CPR	0.091	18	6.9	5.4	6.9	18

^aInitial glycerol concentration: 100 mM. ^bData obtained for 5% conversion. For the APR reactor, the catalyst amount was chosen to obtain light absorbance of ca. 90%.

PAA in water under near-UV, visible, UV-visible and simulated solar light. Very high selectivity values, up to 90%, were found. The results indicated that N-doping improved absorption of visible light by catalysts, but reaction rate did not increase. Selectivity was higher in the presence of less crystallized catalysts, whereas doping seems to have a slightly improving effect. Moreover, the higher selectivities under visible light irradiation could be tentatively explained by the higher energy required by the sites where mineralization occurred with respect to those effective for partial oxidation, although the presence of nitrogen could induce preferential pathways to partial oxidation.

Aliphatic Alcohol Partial Oxidation. From the reactivity results obtained with the aromatic alcohols, the following question arises: are poorly crystallized TiO₂ photocatalysts always efficient to carry out other types of partial oxidations with high performance and selectivity? To answer this question, a study on the partial oxidation of glycerol, an aliphatic polyalcohol, by using two different batch photoreactors, an annular (APR) and a cylindrical (CPR) one, was carried out in water.⁴⁸ The photocatalysts used were both commercial and HP TiO₂ samples.^{25,28} The detected products were: glyceraldehyde (GAD), 1,3-dihydroxyacetone (DHA), formic acid (FA), and carbon dioxide (CO₂). Table 7 shows some selected results obtained with the two reactor configurations. Contrary to the results obtained for the partial oxidation of aromatic alcohols, the most crystalline TiO₂ commercial samples showed the best performances both for alcohol conversion and selectivity toward the corresponding aldehydes. The different behavior probably was due to the various experimental conditions used and to the presence of three OH groups in the molecule of glycerol that could contemporaneously interact on the surface of the photocatalyst. This interaction was more important when the photocatalysts consisted mainly of amorphous phase (high degree of hydroxylation and high specific surface areas). Moreover, the CPR was globally more efficient than the APR because under similar experimental conditions the time required for a conversion of 35% was lower and the selectivity toward the products was higher. The optical thicknesses estimated, at the experimental conditions under which the maximum of selectivity was obtained (catalyst amounts 0.091 and 0.100 g/L for P25, see Table 7), were 3.38 and 2.32 for CPR and APR, respectively.

Partial Oxidation in Harmless Organic Solvents. Even if photocatalytic reactions are often carried out in water, which is the green solvent par excellence, the low solubility in water of

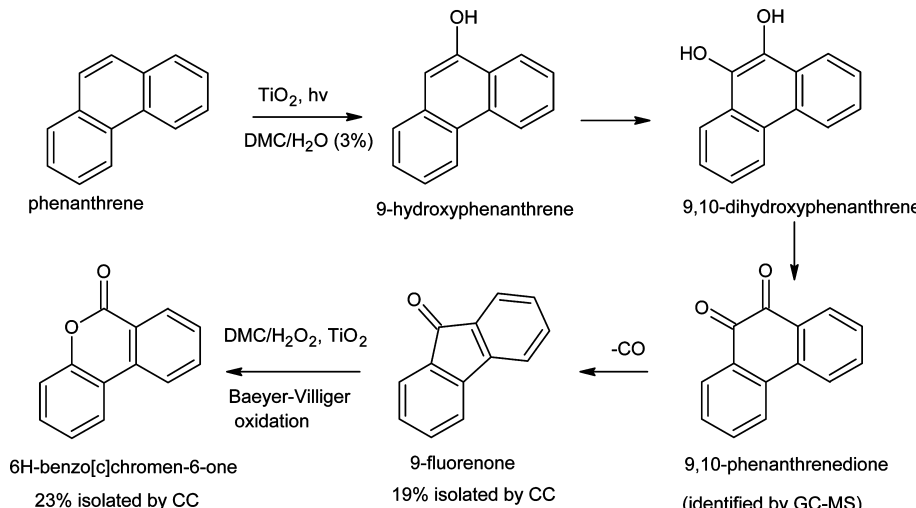
many organic substrates represents a problem for the associated photocatalytic syntheses. The polycyclic aromatic hydrocarbons (PAHs) family is an example of compounds that are insoluble or poorly soluble in water, and their photo-oxidation is reported to occur in solvents as acetonitrile, subcritical water, water-acetone mixtures, and nonionic surfactant solutions. Dimethyl carbonate with a very low amount of water has been proposed as a green organic solvent for the photocatalytic oxidation of phenanthrene.⁴⁹ The experimental runs were carried out in a fixed bed reactor with total recirculation containing Pyrex beads covered by a home prepared TiO₂ film. For comparison purposes, the same reaction was carried out also in ethanol, 1-propanol or 2-propanol, but many products deriving from the interaction between the solvent and the substrate were found. Phenanthrene transformation rate was higher in the presence of a small amount of water, possibly because of the higher production of OH radicals obtained by water oxidation. The use of dimethyl carbonate as the solvent allowed not only to achieve 19% and 23% selectivity toward 9-fluorenone and 6H-benzo[c]chromen-6-one, respectively, but also to avoid byproducts due to solvent-substrate reaction. The proposed reaction pathway is shown in Scheme 3.

Photoelectrocatalytic Syntheses. Photoelectrocatalysis (PEC), that is, the combination of heterogeneous photocatalysis (PC) with electrocatalysis (EC), has shown to be an effective tool for hindering the photogenerated pairs recombination and consequently for improving the yield of partial oxidation reactions.⁵⁰ This method consists in applying an external potential bias to a thin TiO₂ layer deposited on a conductive support.^{51–53}

Photoelectrocatalysis allows working in continuous mode by supporting the semiconductors to the electrode surface, and in the course of the reaction the intermediates do not interact with substrate due to the fact that the anodic and cathodic reactions occur in separate sides.⁵⁴

Photoelectrocatalysis allows working in continuous mode by supporting the semiconductors to the electrode surface, and in

Scheme 3. Proposed Reaction Pathways to 9-Fluorenone and 6H-Benzo[c]chromen-6-one



the course of the reaction the intermediates do not interact with substrate due to the fact that the anodic and cathodic reactions occur in separate sides.⁵⁴ Most of the literature on PEC deals with the degradation of harmful compounds^{55–57} or the water splitting.^{58–61} Only a few works concern the syntheses carried out in water⁵⁰ or organic solvents.^{62,63} Palombari et al.⁶² performed the first PEC synthesis of PAA from 4-MBA in CH₃CN solvent. In this work, anatase and rutile TiO₂/Ti anodes were prepared by thermal and anodic oxidation methods at different temperatures; almost 100% selectivity to PAA was obtained at all the used experimental conditions. The most efficient photocurrent for rutile TiO₂ on Ti samples was obtained with 1 μm thickness of these photoanodes. Mechanistic information on the photo-oxidation of some benzylic derivatives was obtained. In particular, it was observed that, at least with respect to the primary oxidation steps, the reaction mechanisms appeared to be the same as in aqueous medium.

PEC syntheses of benzyl alcohols, ethers, and 1,2-diols carried out in aerated or deaerated CH₃CN solvent by using TiO₂ (rutile)/Ti anodes under UV irradiation have been investigated and the results are summarized in Table 8.⁵⁴ It was hypothesized that (i) an electron transfer to the benzylic radical intermediate occurred within the initial steps, (ii) a second electron transfer from the intermediate benzylic radical to the final product occurred only in the absence of O₂ (in the presence of N₂), and (iii) the radical intermediate was trapped by oxygen and/or it was oxidized to the corresponding cation in aerated medium (oxygen or air).

The current efficiency obtained in the experiments was higher than 70% and the carbon balance was satisfied at ca. 90%.

The PEC oxidation of 4-MBA to PAA has been carried out in water by using TiO₂ (rutile)/Ti anode, prepared by thermal oxidation at 700 °C; some experiments were performed also in CH₃CN. Experiments in water showed a smaller current density (ca. 23%) with respect to CH₃CN (ca. 92%). The PAA yield in water was significantly lower than that in CH₃CN (10% vs 27%).

This reaction has been also performed in water and under UV irradiation by using a three-electrode batch reactor.⁵⁰ TiO₂ films on Ti foil as photoanode were prepared by dip-coating using TiCl₄ as the precursor, followed by calcination (TiO₂/Ti-X) or direct thermal oxidation of Ti foil at 400–700 °C (Ti-X, being X the treatment temperature). The photoanode

preparation method, the calcination temperature and the bias values were optimized to maximize the 4-MBA conversion and the aldehyde selectivity. With a 0.75 V bias versus saturated calomel electrode, very high activities and selectivities were obtained. For instance, by using Ti foil calcined at 500 °C, the initial reaction rate was 0.1507 mM h⁻¹ and the selectivity 85%, whereas by using TiO₂ film prepared by dip-coating and calcined at 700 °C, these values became 0.1339 mM h⁻¹ and 90%, respectively. These results show that the crystalline samples could be useful for the PEC synthesis of aromatic aldehyde in water with high selectivity. This work also showed the effect of the substituent groups of benzyl alcohols on reactivity and selectivity. Benzyl alcohol (BA), 2-methoxybenzyl alcohol (2-MBA), 3-methoxybenzyl alcohol (3-MBA), 2,4-dimethoxybenzyl alcohol (2,4-DMBA), 2,3,4-trimethoxybenzyl alcohol (2,3,4-TMBA), 4-nitrobenzyl alcohol (4-NBA), and 4-hydroxybenzyl alcohol (4-HBA) were used as the substrates. Selected results are reported in Table 9. In the presence of an electron-donor group in para or ortho (or both) position of benzyl alcohol, the alcohol conversion and the selectivity to aldehydes increased.

Titania Photoreactivity: The Importance of Being Amorphous. Since the Fujishima and Honda⁶⁴ discovery of the photocatalytic splitting of water on a TiO₂ electrode under UV light, TiO₂ materials have been widely investigated and applied in energetic and environmental areas. The efficiency of these photocatalysts depends on the effective separation of the photoproduced holes and electrons and the subsequent charge transfer reactions with adsorbed molecules, with these processes being affected by the TiO₂ particle size. When the size of the material is in the nanometer scale, interesting physical and chemical properties emerge.⁶⁵ In fact, in these conditions, the specific surface area and surface-to-volume ratio drastically increases, so that the interaction between the material and the surrounding media is facilitated, and moreover, when the crystal size is comparable with the exciton radius (1–10 nm), the quantum size effect becomes important.

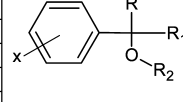
In order to explore the new possibilities offered by nanoparticles, nanocrystalline anatase powders were prepared by TiCl₄ hydrolysis at low temperature.²⁵ XRD investigation of those home prepared (HP) samples revealed that the powders contained anatase phase with small crystal size after 0.5 h aging (HP0.5). The size slightly grew after 2 h (HP2) and it remained

Table 8. Current Efficiency and Conversion of Substrates for PEC by TiO_2 (rutile)/Ti in $\text{CH}_3\text{CN}^{54a}$

substrate	product	conversion (%)	product yield (%) ^a	current efficiency (%) ^b	n ^c
1 (N_2)	4-methoxyacetophenone	40	30	110	2
1 (O_2)	4-methoxyacetophenone	62	30	85	2
2a (N_2)	4-methoxybenzaldehyde	35	25	110	2
2a (O_2)	4-methoxybenzaldehyde (A) 4-methoxybenzoic acid methyl ester (B)	22	13 (A), 6 (B)	105	2 (A), 1 (B)
2b (O_2)	4-methoxybenzoic acid methyl ester (B) 4-methoxyacetophenone (C)	24	9 (C), 6 (B)	110	2 (C), 1 (B)
3a (N_2)	Benzaldehyde	22	18	81	2
3a (O_2)	Benzaldehyde	20	27	80	1
3b (N_2)	Acetophenone	40	26	93	2
3b (O_2)	Acetophenone	30	20	95	1
3c (N_2)	Benzaldehyde	30	28 ^d	90	2
3c (O_2)	Benzaldehyde	30	15 ^a	83	2
3d (N_2)	4-methoxybenzaldehyde	25	13 ^a	82	2
3d (O_2)	4-methoxybenzaldehyde	27	16 ^a	91	2
3e (N_2)	3-methoxybenzaldehyde	6	8 ^a	94	2
3e (O_2)	3-methoxybenzaldehyde	29	21 ^a	85	2
3f (N_2)	4-CF ₃ -benzaldehyde	29	20 ^a	85	2
3f (O_2)	4-CF ₃ -benzaldehyde	25	16 ^a	70 (140)	2 (1)

	X	R	R ₁	R ₂	
1	4-CH ₃ O	CH ₃	H	H	
2a	4-CH ₃ O	H	CH ₃	H	
2b	4-CH ₃ O	CH ₃	CH ₃	H	
3a	H	H	H	CH ₂ OH	
3b	H	CH ₃	H	CH ₂ OH	
3c	H	H	H	PhCHOH	
3d	4-CH ₃ O	H	H	4-CH ₃ OPhCHOH	
3e	3-CH ₃ O	H	H	3-CH ₃ OPhCHOH	
3f	4-CF ₃	H	H	4-CF ₃ PhCHOH	

^aReprinted with permission.⁵⁴ Copyright 2008, Wiley. ^bAccording to the product/substrate stoichiometry (2/1), the reported yield is half of the measured one. ^cError = ± 20 . ^dExchanged electrons per product molecules (1–3b) or with respect to the half of product molecules (3c–3f).

Table 9. Results of Photoelectrocatalytic Oxidations of Substituted Aromatic Alcohols by Using $\text{TiO}_2/\text{Ti-700}$ and Ti-500^a

catalyst	substrate ^b	r_0 [mM·h ⁻¹]	selectivity [%]
$\text{TiO}_2/\text{Ti-700}$	4-MBA	0.1339	90
Ti-500	4-MBA	0.1507	85
$\text{TiO}_2/\text{Ti-700}$	BA	0.0325	13
Ti-500	BA	0.0249	20
$\text{TiO}_2/\text{Ti-700}$	2-MBA	0.1304	60
Ti-500	2-MBA	0.1643	70
$\text{TiO}_2/\text{Ti-700}$	3-MBA	0.0469	9
Ti-500	3-MBA	0.0408	16
$\text{TiO}_2/\text{Ti-700}$	2,4-DMBA	0.2884	54
Ti-500	2,4-DMBA	0.2883	50
$\text{TiO}_2/\text{Ti-700}$	2,3,4-TMBA	0.1042	35
Ti-500	2,3,4-TMBA	0.1024	37
$\text{TiO}_2/\text{Ti-700}$	4-NBA	0.0329	3
Ti-500	4-NBA	0.0469	2
$\text{TiO}_2/\text{Ti-700}$	4-HBA	0.0435	11
Ti-500	4-HBA	0.0314	12

^aInitial degradation rate, r_0 . Selectivity values were determined at 25% conversion. Initial aromatic alcohol concentration, 0.5 mM; bias, 0.75 V. ^bBenzyl alcohol, BA; 2-methoxybenzyl alcohol, 2-MBA; 3-methoxybenzyl alcohol, 3-MBA; 2,4-dimethoxybenzyl alcohol, 2,4-DMBA; 2,3,4-trimethoxybenzyl alcohol 2,3,4-TMBA; 4-nitrobenzyl alcohol, 4-NBA; and 4-hydroxybenzyl alcohol, 4-HBA.

nearly unaltered with further aging, whereas the anatase content decreased and rutile formation increased until almost complete

anatase transformation into rutile after 8 h aging (HP8). For these samples, the percentage of crystalline phases, determined with respect to CaF_2 in ref 66, was in the 5–18% range, indicating that the samples consisted of crystalline and (predominantly) amorphous phases.

The presence of amorphous oxides, whose characterization is very difficult, is usually neglected when the photoreactivity properties of TiO_2 samples are investigated. As an example, most of the investigations carried out with P25 (Degussa) TiO_2 report that this reference photocatalyst is only a mixture of anatase and rutile phases, although the samples of this photocatalyst contain also amorphous phase (up to 13%).⁶⁷ It is acceptable to neglect the amorphous phase when its amount is very low, but it becomes incorrect for important amounts.^{68,69} The finding that for HP samples the growth of the crystal size of the anatase phase was hindered and that the transformation to rutile phase occurred at 373 K (anatase is usually transformed into rutile by calcination at temperatures higher than 873 K) suggests that the significant presence of amorphous TiO_2 affects the interactions among the different components of TiO_2 nanoparticles and eventually the photoactivity performance.

In order to analyze these interactions, the HP samples were subjected to analyses by ¹H-MAS NMR spectroscopy, a technique able to discern the characteristics of the hydroxyls of the different components of the samples,⁷⁰ that is, TiO_2 precursor and very small amorphous and anatase nanoparticles.⁷¹ This investigation indicated that the synthesis in water and the aging treatments at low temperature initially induce the

formation of amorphous TiO_2 and very defective anatase phases. Subsequently, their strong interaction leads to the covering of the anatase surface by the amorphous TiO_2 and this phenomenon hinders the anatase growth favoring the transformation of the metastable anatase into the stable rutile, according to the Ostwald's rule.⁷²

The coexistence and arrangement of crystalline and amorphous phases play an important role in determining the bulk and surface characteristics of the samples with important consequence on the photoactivity of TiO_2 nanoparticles prepared at low temperature.

The coexistence and arrangement of crystalline and amorphous phases play an important role in determining the bulk and surface characteristics of the samples with important consequence on the photoactivity of TiO_2 nanoparticles prepared at low temperature.⁷³ A comparative study of amorphous-rich and amorphous-poor samples was carried out to determine the influence of amorphous phase content on the samples activity; HP0.5, HP2, and BDH TiO_2 (commercial anatase with predominantly crystalline content) samples were tested for the 4-MBA photocatalytic oxidation in water.^{25,35}

The performances of the samples were evaluated by determining the kinetic constant of the 4-MBA disappearance rate (a parameter related to the rate of photon absorption, which is a phenomenon mainly occurring in the sample bulk) and the selectivity toward the partial oxidation product (a parameter related to the substrate adsorption onto the sample surface area). The 4-MBA disappearance rate ($-r_{4\text{-MBA}}$) obeys first-order kinetics with respect to 4-MBA concentration

$$(-r_{4\text{-MBA}}) \equiv -\frac{1}{S} \frac{dN}{dt} = -\frac{V}{S} \frac{dC}{dt} = kC$$

in which S is the surface area of the catalyst, N the 4-MBA moles, t the irradiation time, V the reaction volume, C the 4-MBA concentration, and k is the first-order kinetic constants of MBA transformation reaction. Table 10 reports the figures of this

Table 10. Features of Anatase TiO_2 Samples and Their Performance in the 4-MBA Photocatalytic Oxidation to Aldehyde

catalyst	SSA ^a [m^2/g]	AT [%]	$k \cdot 10^6$ ^b [m/h]	selectivity [%]
HP0.5	235	94	2.73	41
HP2	226	93	3.24	37
BDH	9	5	84.5	6

^aSSA, specific surface area; AT, amorphous TiO_2 ; k , degradation.

^bKinetic constant for alcohol conversion ca. 50%.

kinetic constant together with the reaction selectivity toward aldehyde and some features of the tested samples. The kinetic constant value is normalized with respect to the catalyst surface area. Owing to the fact that the photoreactivity runs were carried out at equal irradiation and reaction conditions, the only difference being the ratio of the amorphous to crystalline

phases of the catalysts, it is justified to take the k value as a reliable parameter for ordering the intrinsic activity of catalysts.

The increase of the reaction rate with the decrease of the amorphous TiO_2 content indicates that the amorphous component, mainly concentrated at the anatase particles contact zones, hampers the photoreactivity by hindering the electron–hole pairs mobility.⁷³ In photocatalytic reactions, the contribution of the interparticles charge transfer is very important, as demonstrated in investigations on the electrons mobility in mesoporous TiO_2 photoanodes⁷⁴ and in catalysts where TiO_2 is used as a support synergistically with metals.^{75–78} The lower reaction rate on HP0.5 than on HP2 indicates that the enhancement of the photocatalytic reaction is determined by the anatase crystallinity improvement, responsible for the decrease of the crystalline defects (where photogenerated electrons and holes recombine) and by the increase in amorphous TiO_2 chains condensation at the contact zone of contiguous anatase particles.

The significantly lower selectivity on TiO_2 BDH (a low defective anatase) than on HP0.5 and HP2 samples indicates that the active sites for 4-MBA partial oxidation are mainly located on the amorphous-anatase TiO_2 interface. These sites, where 4-MBA is adsorbed through the alcoholic group with the aromatic ring plane perpendicular to the surface, probably are strongly basic amorphous TiO_2 terminal hydroxyls bound to low-coordinated Ti^{4+} cations, and they could limit the electron mobility by acting as electron trapping sites in the grains boundaries.⁷⁹ The reaction of 4-MBA alcoholic groups with those hydroxyls should lead first to water formation so that the subtraction of hydrogen atoms from alcoholic groups can facilitate the bonding of these carbon atoms with O_2^- anions of deprotonated amorphous TiO_2 bridging hydroxyls.⁸⁰ As those anions are the favored sites for holes trapping, the reaction of the adsorbed complex with radicals formed by UV irradiation in the presence of O_2 can lead to PAA formation. The lower selectivity on HP2 than on HP0.5 is consistent with the decreasing basic character of the amorphous TiO_2 terminal hydroxyls with increasing condensation of its chains.

The importance of the amorphous phase for TiO_2 photoreactivity has been outlined in a recent study of the anatase nanocrystals surface; it has been demonstrated that when TiO_2 is exposed to light and water vapor, the initially crystalline surface converts to an amorphous phase whose thickness ranges between one and two monolayers.⁸¹ The amorphous layer results from direct photoreaction between the top monolayers of the anatase crystal surface and the adsorbed water. The heavily hydroxylated amorphous layer is stable and does not increase in thickness with time; this disordered layer is presumed to be present on the anatase surface under reaction conditions.

The main result of this investigation is that amorphous TiO_2 plays a very important role in determining the photoreactivity performances of the samples. Many questions, however, remain open; for example it is important to determine the active species responsible for reactivity (surface trapped hole or reactive oxygen) and the real factors affecting the selectivity (the slow electron–hole diffusion in amorphous component or the different surface holes/defects energetic features). The importance of amorphous phase is of general concern in nanoparticles prepared at low temperature; in these conditions, amorphous oxide is always present in the samples and it drastically affects their bulk and surface properties. To ignore its presence may

determine mistakes and misunderstandings in explaining physicochemical properties of the materials.

Issues and Challenges. This article has critically discussed heterogeneous photocatalysis and photoelectrocatalysis as alternative methods for selective syntheses of organic molecules. Some examples have been reported and the photo-oxidation of aromatic alcohols to the corresponding aldehydes in the presence of various TiO₂ samples appears a promising reaction in view of application purposes. Some issues, however, exist and the most important ones are related to the low selectivity of heterogeneous photocatalysis because almost all the organic molecules are attacked and completely degraded by oxidant radicals produced by illumination of the photocatalyst in the presence of O₂. This fact is positive for the photomineralization of noxious species, whereas it is a drawback when it is required to address the reaction toward some specific product(s), in particular toward partial oxidized species. Other weaknesses are the low solubility of most of the organic molecules in H₂O, the consequent low concentration of the reactant species that limits the obtainable reaction rate and the difficulty to recover the product(s).

Therefore, green solvents such as dimethyl carbonate were considered, as for instance in the photo-oxidation of phenanthrene with just small beneficial amounts of water.

Another challenge for the development of heterogeneous photocatalysis could be its coupling with membrane technology. For instance, it has been found that some selected pervaporation membranes are able to permeate selectively vanillin and other aromatic aldehydes. The recovery of the products directly from the reaction environment appears to be a solution to avoid their further transformation. It is likely that also other membrane processes, such as dialysis, can be used to the same aim.

The use of heterogeneous photocatalysis for syntheses is in its infancy and investigations are needed to answer many open questions. It should be emphasized, for instance, that the selectivity of the chosen photocatalyst is related to the type of reaction and the experimental conditions under which the reaction is carried out. Indeed, poorly crystallized TiO₂ photocatalysts (in the anatase, rutile and brookite phases) showed to be quite selective for the photo-oxidation of some aromatic alcohols to the corresponding aldehydes, whereas commercial well crystallized TiO₂ samples (in the anatase and rutile phases) showed to be more selective for glycerol photo-oxidation. As far as TiO₂ is concerned, characterization studies indicate that the effects of interactions between amorphous and crystalline oxides are important to explain the different behavior observed. In particular, it is essential to determine the active species responsible for the photoactivity.

Also, the photoreactor configuration can play a role. An efficient irradiation and a proper photocatalyst amount can increase both conversions and selectivities toward the desired products. A main parameter that must be optimized to maximize the system performances is the optical thickness, which depends on the optical properties of the photocatalyst, on its concentration, and on the geometrical thickness of the reactor.

As far as photoelectrocatalysis is concerned, only a few papers have been published aimed at producing chemicals. This technology looks to be convenient only when a suitable choice of the electrodes is made. Actually, the occurrence of the reduction and oxidation photoreactions in separated sides is positive, but the difficulty of working in aqueous environments is of course an issue.

In conclusion, the presented methods appear to be really promising, but further thorough investigations are needed to address the issues previously illustrated.

AUTHOR INFORMATION

Corresponding Author

*E-mail: leonardo.palmisano@unipa.it. Phone: +39 091 23863746. Mobile: +39 320 4328571. Address: University of Palermo, DEIM, Viale delle Scienze, Building 6, 90128 Palermo, Italy.

Notes

The authors declare no competing financial interest.

Biographies

Vincenzo Augugliaro is Full Professor of Transport Phenomena at the University of Palermo (Italy). He contributed to the following fields: chemical absorption kinetics, biochemical reactor modeling, diffusional kinetics in metalliding alloys, chemical kinetics of heterogeneous photocatalytic systems, modeling of heterogeneous photoreactors, radiation field modeling in absorbing-reacting media, advanced oxidation processes. <http://www.unipa.it/photocatalysis/profili.php>.

Giovanni Camera-Roda is Associate Professor at the University of Bologna (Italy). He used a chemical engineering approach in different fields as transport phenomena, photocatalytic reactions, membrane separation and radiant energy transport. He has been recently involved in “process intensification”, aiming to improve yield and sustainability of chemical and physical transformations. <http://www.unibo.it/docenti/giovanni.cameraroda>.

Vittorio Loddo is currently Associate Professor of Transport Phenomena at the University of Palermo (Italy). He has contributed to the following fields: chemical kinetics of heterogeneous photocatalytic systems, modelling of heterogeneous photoreactors, radiation field modelling in absorbing-reacting media, advanced oxidation processes for environment remediation, and green synthesis. <http://www.unipa.it/photocatalysis/profili.php>.

Giovanni Palmisano is Assistant Professor at Masdar Institute of Science and Technology in Abu Dhabi (UAE). Research activities concern photocatalytic processes, hydrogen production, self-cleaning coatings, and water and air remediation, with attention to materials characterization, kinetics, modelling of photoreactors and radiant fluxes. He is also involved in organic and hybrid photovoltaics. <https://www.masdar.ac.ae/faculty-top/list-of-faculty/item/6373-giovanni-palmisano>.

Leonardo Palmisano is Full Professor of Chemistry at the University of Palermo (Italy). His scientific activity has been mainly focussed on the field of heterogeneous photocatalysis, and his research work deals with various topics concerning preparation, characterisation with bulk and surface techniques, and testing of various bare and doped photocatalysts. <http://www.unipa.it/photocatalysis/profili.php>.

Javier Soria is professor at the Consejo Superior de Investigaciones Científicas, CSIC (Spain). Most of research work has been devoted to the study of the catalysts properties using spectroscopic techniques, mainly electron paramagnetic resonance (EPR) and infrared (FTIR) spectroscopies. The most recurrent field of his research efforts is heterogeneous photocatalysis. <http://www.energy.imdea.org/about-us/scientific-council>.

Sedat Yurdakal is Associate Professor at the University of Afyon Kocatepe (Turkey). His research activity is in the field heterogeneous photocatalysis, such as selective photocatalytic and photoelectrocatalytic oxidations, remediation of harmful compounds, thin films, photocatalytic reactor applications, photoadsorption determination and preparation of new materials containing TiO₂. <http://www.akademi.aku.edu.tr/frmCvler.aspx?ID=83JQM92NDAU853971AQ101>.

ACKNOWLEDGMENTS

S. Yurdakal thanks to TÜBİTAK (Project no: 111T489) for economic support. Authors thank Cosimo D'Amico (Palermo, Italy, cosimodamico58@libero.it) for cover production.

REFERENCES

- (1) Photoelectrochemistry, Photocatalysis and Photoreactors. *Fundamentals and Developments*; Schiavello, M., Ed.; Reidel: Dordrecht, Netherlands, 1985.
- (2) Augugliaro, V.; Palmisano, L.; Sclafani, A.; Minero, C.; Pelizzetti, E. Photocatalytic Degradation of Phenol in Aqueous Titanium Dioxide Dispersion. *Toxicol. Environ. Chem.* **1988**, *16*, 89–109.
- (3) Serpone, N.; Pelizzetti, E., Eds. *Photocatalysis, Fundamentals and Applications*; Wiley: New York, 1989.
- (4) Ollis, D. F.; Al-Ekabi, H. *Photocatalytic Purification and Treatment of Water and Air*; Elsevier: New York, 1993.
- (5) Hoffmann, M. R.; Martin, S. T.; Choi, W.; Bahnemann, D. W. Environmental Applications of Semiconductor Photocatalysis. *Chem. Rev.* **1993**, *93*, 69–96.
- (6) Legrini, O. R.; Oliveros, E.; Brown, A. Photocatalytic Processes for Water Treatment. *Chem. Rev.* **1993**, *93*, 671–698.
- (7) Augugliaro, V.; Coluccia, S.; Loddo, V.; Marchese, L.; Martra, G.; Palmisano, L.; Schiavello, M. Photocatalytic Oxidation of Gaseous Toluene on Anatase TiO₂ Catalyst: Mechanistic Aspects and FT-IR Investigation. *Appl. Catal., B* **1999**, *20*, 15–27.
- (8) Fujishima, A.; Rao, T. N.; Tryk, D. A. Titanium Dioxide Photocatalysis. *J. Photochem. Photobiol. C: Photochem. Rev.* **2000**, *1*, 1–21.
- (9) Kamat, P. V.; Meisel, D. Nanoparticles in Advanced Oxidation Processes. *Curr. Opin. Colloid Interface Sci.* **2002**, *7*, 282–287.
- (10) Fox, M. A.; Dulay, M. T. Heterogeneous Photocatalysis. *Chem. Rev.* **1993**, *93*, 341–357.
- (11) Mahdavi, F.; Bruton, T. C.; Li, Y. Photoinduced Reduction of Nitro Compounds on Semiconductor Particles. *J. Org. Chem.* **1993**, *58*, 744–746.
- (12) Palmisano, G.; García López, E.; Marci, G.; Loddo, V.; Yurdakal, S.; Augugliaro, V.; Palmisano, L. Advances in Selective Conversions by Heterogeneous Photocatalysis. *Chem. Commun.* **2010**, *46*, 7074–7089.
- (13) Palmisano, L.; Augugliaro, V.; Bellardita, M.; Di Paola, A.; García López, E.; Loddo, V.; Marci, G.; Palmisano, G.; Yurdakal, S. Titania Photocatalysts for Selective Oxidations in Water. *ChemSusChem* **2011**, *4*, 1431–1438.
- (14) Lang, X.; Chen, X.; Zhao, J. Heterogeneous Visible Light Photocatalysis for Selective Organic Transformations. *Chem. Soc. Rev.* **2014**, *43*, 473–486.
- (15) Ohtani, B.; Pal, B.; Ikeda, S. Photocatalytic Organic Syntheses: Selective Cyclization of Amino Acids in Aqueous Suspensions. *Catal. Surv. Asia* **2003**, *7*, 165–176.
- (16) Sahle-Demessie, E.; Gonzalez, M.; Wang, Z.; Biswas, P. Synthesizing Alcohols and Ketones by Photoinduced Catalytic Partial Oxidation of Hydrocarbons in TiO₂ Film Reactors Prepared by Three Different Methods. *Indus. Eng. Chem. Res.* **1999**, *38*, 3276–3284.
- (17) Almquist, C. B.; Biswas, P. The Photo-oxidation of Cyclohexane on Titanium Dioxide: an Investigation of Competitive Adsorption and its Effects on Product Formation and Selectivity. *Appl. Catal., A* **2001**, *214*, 259–271.
- (18) Li, N.; Lang, X.; Ma, W.; Ji, H.; Chen, C.; Zhao, J. Selective Aerobic Oxidation of Amines to Imines by TiO₂ Photocatalysis in Water. *Chem. Commun.* **2013**, *49*, 5034–5036.
- (19) Cermenati, L.; Dondi, D.; Fagnoni, M.; Albini, A. Titanium Dioxide Photocatalysis of Adamantane. *Tetrahedron* **2003**, *59*, 6409–6414.
- (20) Caronna, T.; Gambarotti, C.; Palmisano, L.; Punta, C.; Recupero, F. Sunlight-Induced Reactions of Some Heterocyclic Bases with Ethers in the Presence of TiO₂. A Green Route for the Synthesis of Heterocyclic Aldehydes. *J. Photochem. Photobiol., A* **2005**, *171*, 237–242.
- (21) Pillai, U. R.; Sahle-Demessie, E. Selective Oxidation of Alcohols in Gas Phase Using Light-Activated Titanium Dioxide. *J. Catal.* **2002**, *211*, 434–444.
- (22) Mohamed, O. S.; El-Aal, A.; Gaber, M.; Abdel-Wahab, A. A. Photocatalytic Oxidation of Selected Aryl Alcohols in Acetonitrile. *J. Photochem. Photobiol., A* **2002**, *148*, 205–210.
- (23) Anastas, P.; Eghbali, N. Green Chemistry: Principles and Practice. *Chem. Soc. Rev.* **2010**, *39*, 301–312.
- (24) Camera Roda, G.; Augugliaro, V.; Loddo, V.; Palmisano, L. Pervaporation Membrane Reactors. In *Handbook of Membrane Reactors*, Vol. 1; Basile, A., Ed., Woodhead Publishing: Cambridge, U.K., 2013; pp 107–149.
- (25) Palmisano, G.; Yurdakal, S.; Augugliaro, V.; Loddo, V.; Palmisano, L. Photocatalytic Selective Oxidation of 4-Methoxybenzyl Alcohol to Aldehyde in Aqueous Suspension of Home-Prepared Titanium Dioxide Catalyst. *Adv. Synth. Catal.* **2007**, *349*, 964–970.
- (26) Loddo, V.; Yurdakal, S.; Palmisano, G.; Imoberdorf, G. E.; Irazoqui, H. A.; Alfano, O. M.; Augugliaro, V.; Berber, H.; Palmisano, L. Selective Photocatalytic Oxidation of 4-Methoxybenzyl Alcohol to p-Anisaldehyde in Organic-Free Water in a Continuous Annular Fixed Bed Reactor. *Int. J. Chem. React. Eng.* **2007**, *5*, A57.
- (27) Yurdakal, S.; Loddo, V.; Palmisano, G.; Augugliaro, V.; Berber, H.; Palmisano, L. Kinetics of 4-methoxybenzyl Alcohol Oxidation in Aqueous Solution in a Fixed Bed Photocatalytic Reactor. *Ind. Eng. Chem. Res.* **2010**, *49*, 6699–6708.
- (28) Yurdakal, S.; Palmisano, G.; Loddo, V.; Alagöz, O.; Augugliaro, V.; Palmisano, L. Selective Photocatalytic Oxidation of 4-Substituted Aromatic Alcohols in Water with Rutile TiO₂ Prepared at Room Temperature. *Green Chem.* **2009**, *11*, 510–516.
- (29) Addamo, M.; Augugliaro, V.; Di Paola, A.; García López, E.; Loddo, V.; Marci, G.; Molinari, R.; Palmisano, L.; Schiavello, M. Preparation, Characterization, and Photoactivity of Polycrystalline Nanostructured TiO₂ Catalysts. *J. Phys. Chem. B* **2004**, *108*, 3303–3310.
- (30) Nag, M.; Basak, P.; Manorama, S. V. Low Temperature Hydrothermal Synthesis of Phase-Pure Rutile Titania Nanocrystals: Time Temperature Tuning of Morphology and Photocatalytic Activity. *Mater. Res. Bull.* **2007**, *42*, 1691–1704.
- (31) Yurdakal, S.; Palmisano, G.; Loddo, V.; Augugliaro, V.; Palmisano, L. Nanostructured Rutile TiO₂ for Selective Photocatalytic Oxidation of Aromatic Alcohols to Aldehydes in Water. *J. Am. Chem. Soc.* **2008**, *130*, 1568–1569.
- (32) Augugliaro, V.; Caronna, T.; Loddo, V.; Marci, G.; Palmisano, G.; Palmisano, L.; Yurdakal, S. Oxidation of Aromatic Alcohols in Irradiated Aqueous Suspensions of Commercial and Home Prepared Rutile TiO₂: A Selectivity Study. *Chem.—Eur. J.* **2008**, *14*, 4640–4646.
- (33) Augugliaro, V.; Kisch, H.; Loddo, V.; López-Muñoz, M. J.; Márquez-Alvarez, C.; Palmisano, G.; Palmisano, L.; Parrino, F.; Yurdakal, S. Photocatalytic Oxidation of Aromatic Alcohols to Aldehydes in Aqueous Suspension of Home Prepared Titanium Dioxide 2. Intrinsic and Surface Features of Catalysts. *Appl. Catal., A* **2008**, *349*, 189–197.
- (34) Roy, A. M.; De, G. C.; Sasimal, N.; Bhattacharyya, S. S. Determination of the Flat Band Potential of Semiconductor Particles in Suspension by Photovoltage Measurements. *Int. J. Hydrogen Energy* **1995**, *20*, 627–630.
- (35) Augugliaro, V.; Kisch, H.; Loddo, V.; López-Muñoz, M. J.; Márquez-Alvarez, C.; Palmisano, G.; Palmisano, L.; Parrino, F.; Yurdakal, S. Photocatalytic Oxidation of Aromatic Alcohols to Aldehydes in Aqueous Suspension of Home-Prepared Titanium Dioxide 1. Selectivity Enhancement by Aliphatic Alcohols. *Appl. Catal. A: Gen.* **2008**, *349*, 182–188.
- (36) Augugliaro, V.; Loddo, V.; López-Muñoz, M. J.; Márquez-Alvarez, C.; Palmisano, G.; Palmisano, L.; Yurdakal, S. Home-Prepared Anatase, Rutile, and Brookite TiO₂ for Selective Photocatalytic Oxidation of 4-Methoxybenzyl Alcohol in Water: Reactivity and ATR-FTIR study. *Photochem. Photobiol. Sci.* **2009**, *8*, 663–669.

- (37) Yurdakal, S.; Augugliaro, V. Partial Oxidation of Aromatic Alcohols via TiO_2 Photocatalysis: The Influence of Substituent Groups on the Activity and Selectivity. *RSC Adv.* **2012**, *2*, 8375–8380.
- (38) Karabacak, B.; Erdem, M.; Yurdakal, S.; Çimen, Y.; Türk, H. Facile Two-Step Preparation of Polystyrene/Anatase TiO_2 Core/Shell Colloidal Particles and Their Potential Use as an Oxidation Photocatalyst. *Mater. Chem. Phys.* **2014**, *144*, 498–504.
- (39) Yurdakal, S.; Tek, B. S.; Alagöz, O.; Augugliaro, V.; Loddo, V.; Palmisano, G.; Palmisano, L. Photocatalytic Selective Oxidation of 5-(Hydroxymethyl)-2-Furaldehyde to 2,5-Furandicarbaldehyde in Water by Using Anatase, Rutile, and Brookite TiO_2 Nanoparticles. *ACS Sustainable Chem. Eng.* **2013**, *1*, 456–461.
- (40) Bellardita, M.; Loddo, V.; Palmisano, G.; Pibiri, I.; Palmisano, L.; Augugliaro, V. Photocatalytic Green Synthesis of Piperonal in Aqueous TiO_2 Suspension. *Appl. Catal., B* **2014**, *144*, 607–613.
- (41) Augugliaro, V.; Camera Roda, G.; Loddo, V.; Palmisano, G.; Palmisano, L.; Parrino, F.; Puma, M. A. Synthesis of Vanillin in Water by TiO_2 Photocatalysis. *Appl. Catal., B* **2012**, *111–112*, 555–561.
- (42) Camera Roda, G.; Santarelli, F.; Augugliaro, V.; Loddo, V.; Palmisano, G.; Palmisano, L.; Yurdakal, S. Photocatalytic Process Intensification by Coupling with Pervaporation. *Catal. Today* **2011**, *161*, 209–213.
- (43) Camera Roda, G.; Augugliaro, V.; Cardillo, A.; Loddo, V.; Palmisano, G.; Palmisano, L. A Pervaporation Photocatalytic Reactor for the Green Synthesis of Vanillin. *Chem. Eng. J.* **2013**, *224*, 136–143.
- (44) Camera Roda, G.; Augugliaro, V.; Loddo, V.; Palmisano, G.; Palmisano, L. Production of Aldehydes by Oxidation in Aqueous Medium with Selective Recovery of the Product by Means of Pervaporation. WIPO Patent WO2011154925A1; U.S. Patent US20130123546; European Patent EP2580182A1.
- (45) Sivaranjani, K.; Gopinath, C. Porosity Driven Photocatalytic Activity of Wormhole Mesoporous $\text{TiO}_{2-x}\text{N}_x$ in Direct Sunlight. *J. Mater. Chem.* **2011**, *21*, 2639–2647.
- (46) Yurdakal, S.; Augugliaro, V.; Loddo, V.; Palmisano, G.; Palmisano, L. Enhancing Selectivity in Photocatalytic Formation of *p*-Anisaldehyde in Aqueous Suspension Under Solar Light Irradiation via TiO_2 N-Doping. *New J. Chem.* **2012**, *36*, 1762–1768.
- (47) Tek, B. S.; Yurdakal, S.; Özcan, L.; Augugliaro, V.; Loddo, V.; Palmisano, G. N-doped Anatase-Rutile Photocatalysts for Aromatic Aldehyde Synthesis under UV and Solar Irradiation. *Sci. Adv. Mater.* **2015**, DOI: 10.1166/sam.2015.2280.
- (48) Augugliaro, V.; Hamed El Nazer, H. A.; Loddo, V.; Mele, A.; Palmisano, G.; Palmisano, L.; Yurdakal, S. Partial Photocatalytic Oxidation of Glycerol in TiO_2 Water Suspensions. *Catal. Today* **2010**, *151*, 21–28.
- (49) Bellardita, M.; Loddo, V.; Mele, A.; Panzeri, W.; Parrino, F.; Pibiri, I.; Palmisano, L. Photocatalysis in Dimethyl Carbonate Green Solvent: Degradation and Partial Oxidation of Phenanthrene on Supported TiO_2 . *RSC Adv.* **2014**, *4*, 40859–40864.
- (50) Özcan, L.; Yurdakal, S.; Augugliaro, V.; Loddo, V.; Palmas, S.; Palmisano, G.; Palmisano, L. Photoelectrocatalytic Selective Oxidation of 4-Methoxybenzyl Alcohol in Water by TiO_2 Supported on Titanium Anodes. *Appl. Catal., B* **2013**, *132–133*, 535–542.
- (51) Rajeshwar, K. Photoelectrochemistry and the Environment. *J. Appl. Electrochem.* **1995**, *25*, 1067–1082.
- (52) Palmisano, G.; Loddo, V.; El Nazer, H. H.; Yurdakal, S.; Augugliaro, V.; Ciriminna, R.; Pagliaro, M. Graphite-Supported TiO_2 for 4-Nitrophenol Degradation in a Photoelectro-catalytic Reactor. *Chem. Eng. J.* **2009**, *155*, 339–346.
- (53) Samiolo, L.; Valigi, M.; Gazzoli, D.; Amadelli, R. Photo-electro Catalytic Oxidation of Aromatic Alcohols on Visible Light-Absorbing Nitrogen-Doped TiO_2 . *Electrochim. Acta* **2010**, *55*, 7788–7795.
- (54) Bettoni, M.; Rol, C.; Sebastiani, G. V. Photoelectrochemistry on TiO_2/Ti Anodes as a Tool to Increase the Knowledge About Some Photo-oxidation Mechanisms in CH_3CN . *J. Phys. Org. Chem.* **2008**, *21*, 219–224.
- (55) Chai, S.; Zhao, G.; Li, P.; Lei, Y.; Zhang, Y.; Li, D. Novel Sieve-Like $\text{SnO}_2/\text{TiO}_2$ Nanotubes with Integrated Photoelectrocatalysis: Fabrication and Application for Efficient Toxicity Elimination of Nitrophenol Wastewater. *J. Phys. Chem. C* **2011**, *115*, 18261–18269.
- (56) Scott-Emuakpor, E. O.; Kruth, A.; Todd, M. J.; Raab, A.; Paton, G. I.; Macphee, D. E. Remediation of 2,4-Dichlorophenol Contaminated Water by Visible Light-Enhanced WO_3 Photoelectrocatalysis. *Appl. Catal. B: Environ.* **2012**, *123–124*, 433–439.
- (57) Li, K.; Zhang, H.; Tang, T.; Xu, Y.; Ying, D.; Wang, Y.; Jia, J. Optimization and Application of $\text{TiO}_2/\text{Ti}-\text{Pt}$ Photo Fuel Cell (PFC) to Effectively Generate Electricity and Degrade Organic Pollutants Simultaneously. *Water Res.* **2014**, *62*, 1–10.
- (58) Mirbagheri, N.; Wang, D.; Peng, C.; Wang, J.; Huang, Q.; Fan, C.; Ferapontova, E. E. Visible Light Driven Photoelectrochemical Water Oxidation by Zn- and Ti-Doped Hematite Nanostructures. *ACS Catal.* **2014**, *4*, 2006–2015.
- (59) Kajita, M.; Saito, K.; Abe, N.; Shoji, A.; Matsubara, K.; Yui, T.; Yagi, M. Visible-Light-Driven Water Oxidation at a Polychromium-Oxo-Electrodeposited TiO_2 Electrode as a New Type of Earth-Abundant Photoanode. *Chem. Commun.* **2014**, *50*, 1241–1243.
- (60) Pitman, C. L.; Miller, A. J. M. Molecular Photoelectrocatalysts for Visible Light-Driven Hydrogen Evolution from Neutral Water. *ACS Catal.* **2014**, *4*, 2727–2733.
- (61) Yu, X.; Han, X.; Zhao, Z.; Zhang, J.; Guo, W.; Pan, C.; Li, A.; Liu, H.; Lin Wang, Z. Hierarchical TiO_2 Nanowire/Graphite Fiber Photoelectrocatalysis Setup Powered by a Wind-Driven Nanogenerator: A Highly Efficient Photoelectrocatalytic Device Entirely Based on Renewable Energy. *Nano Energy* **2015**, *11*, 19–27.
- (62) Palombari, R.; Ranchella, M.; Rol, C.; Sebastiani, G. V. Oxidative Photoelectrochemical Technology with Ti/TiO_2 Anodes. *Sol. Energy Mater. Sol. C* **2002**, *71*, 359–368.
- (63) Bettoni, M.; Meniconi, S.; Rol, C.; Sebastiani, G. V. Selective Photocatalytic Oxidation at TiO_2/Ti Anodes of 4-Methoxybenzyl Alcohol to the Corresponding Benzaldehyde in Green Conditions. *J. Photochem. Photobiol. A: Chem.* **2011**, *222*, 180–184.
- (64) Fujishima, A.; Honda, K. Electrochemical Photolysis of Water at a Semiconductor Electrode. *Nature* **1972**, *238*, 37–38.
- (65) Chen, X.; Mao, S. S. Titanium Dioxide Nanomaterials: Synthesis, Properties, Modifications, and Applications. *Chem. Rev.* **2007**, *107*, 2891–2959.
- (66) Jensen, H.; Joensen, K. D.; Jørgensen, J.-E.; Pedersen, J. S.; Søgaard, E. G. J. Characterization of Nanosized Partly Crystalline Photocatalysts. *Nanoparticle Res.* **2004**, *6*, 519–526.
- (67) Ohtani, B.; Prieto-Mahaney, O. O.; Li, D.; Abe, R. What is Degussa (Evonik) P25? Crystalline Composition Analysis, Reconstruction from Isolated Pure Particles and Photocatalytic Activity Test. *J. Photochem. Photobiol. A* **2010**, *216*, 179–182.
- (68) Zhang, H.; Banfield, J. F. Kinetics of Crystallization and Crystal Growth of Nanocrystalline Anatase in Nanometer-sized Amorphous Titania. *Chem. Mater.* **2002**, *14*, 4145–4154.
- (69) Maira, A. J.; Yeung, K. L.; Lee, C. Y.; Yue, P. L.; Chan, C. K. Size Effects in Gas-Phase Photo-Oxidation of Trichloroethylene Using Nanometer-Sized TiO_2 Catalysts. *J. Catal.* **2000**, *192*, 185–196.
- (70) Pang, W. K.; Low, I. M.; Hanna, J. V. Characterisation of Amorphous Silica in Air-Oxidised Ti_3SiC_2 at 500–1000 °C Using Secondary-Ion Mass Spectrometry, Nuclear Magnetic Resonance and Transmission Electron Microscopy. *Mater. Chem. Phys.* **2010**, *121*, 453–458.
- (71) Sanz, J.; Soria, J.; Sobrados, I.; Yurdakal, S.; Augugliaro, V. Influence of Amorphous TiO_{2-x} on Titania Nanoparticles Growth and Anatase-to-Rutile Transformation. *J. Phys. Chem. C* **2012**, *116*, 5110–5115.
- (72) Ostwald, W. Z. Studies on the Formation and Transformation of Solid Bodies. *Z. Phys. Chem.* **1897**, *22*, 289–330.
- (73) Yurdakal, S.; Augugliaro, V.; Sanz, J.; Soria, J.; Sobrados, I.; Torralvo, M. J. The Influence of the Anatase Nanoparticles Boundaries on the Titania Activity Performance. *J. Catal.* **2014**, *309*, 97–104.
- (74) Docampo, P.; Guldin, S.; Steiner, U.; Snaith, H. J. Charge Transport Limitations in Self-Assembled TiO_2 Photoanodes for Dye-Sensitized Solar Cells. *J. Phys. Chem. Lett.* **2013**, *4*, 698–703.

- (75) Zhang, Y.; Cui, X.; Shi, F.; Deng, Y. Nano-Gold Catalysis in Fine Chemical Synthesis. *Chem. Rev.* **2012**, *112*, 2467–2505.
- (76) Menezes, W. G.; Zielasek, V.; Thiel, K.; Hartwig, A.; Bäumer, M. Effects of Particle Size, Composition, and Support on Catalytic Activity of AuAg Nanoparticles Prepared in Reverse Block Copolymer Micelles as Nanoreactors. *J. Catal.* **2013**, *299*, 222–231.
- (77) Solymosi, F.; Tombácz, I.; Koszta, J. Effects of Variation of Electric Properties of TiO₂ Support on Hydrogenation of CO and CO₂ over Rh catalysts. *J. Catal.* **1985**, *95*, 578–586.
- (78) Berkó, A.; Balázs, N.; Kassab, G.; Óvári, L. Segregation of K and Its Effects on the Growth, Decoration, and Adsorption Properties of Rh Nanoparticles on TiO₂(110). *J. Catal.* **2012**, *289*, 179–189.
- (79) Richter, C.; Schmuttenmaer, C. A. Exciton-Like Trap States Limit Electron Mobility in TiO₂ Nanotubes. *Nat. Nanotechnol.* **2010**, *5*, 769–772.
- (80) Haber, J.; Tokarz, R.; Witko, M. Quantum-Chemical Description of the Oxidation of Alkylnaromatic Molecules on Vanadium Oxide Catalysts. *Stud. Surf. Sci. Catal.* **1994**, *82*, 739–748.
- (81) Zhang, L.; Miller, B. K.; Crozier, P. A. Atomic Level In Situ Observation of Surface Amorphization in Anatase Nanocrystals During Light Irradiation in Water Vapor. *Nano Lett.* **2013**, *13*, 679–684.